

On Feedback Resonant Drift and Interaction with the Boundaries in Circular and Annular Excitable Media[★]

E.V. Nikolaev^{a,b} V.N. Biktashev^{a,b} and A.V. Holden^{a,1}

^a *Department of Physiology, University of Leeds, Leeds LS2 9JT, UK*

^b *Institute for Mathematical Problems in Biology, Pushchino, Moscow Region, 142292, Russia*

Resonant drift has been proposed as a means of controlling cardiac arrhythmias. We study resonant drift in circular and annular media in which it is induced by (1) forcing at a fixed frequency (2) feedback controlled by the orientation of the tip of the spiral wave and (3) feedback controlled *via* monitoring the arrival of the wavefront at a recording point. Trapping resonantly drifting spirals by the holes, their freezing at a fixed site at the outer boundary or in contrast their detaching from the outer boundary produced by the interaction between the resonantly drifting spiral and holes and boundaries are described and explained.

1 Introduction

Re-entrant cardiac arrhythmias can be idealized as spiral wave or scroll wave solutions of reaction-diffusion equations of excitable media, see Holden, Markus and Othmer [17]; Panfilov and Holden [21]. The elimination of such arrhythmias, or the defibrillation of heart muscle, is a vitally important problem, as re-entrant activity in ventricular muscle can be lethal. Biktashev and Holden [5]-[7], Biktashev [4] have proposed exploiting resonant drift of spiral wave position, produced by low amplitude forcing under feedback control (to overcome effects of boundaries and inhomogeneities) to defibrillate cardiac tissue by gently pushing out re-entrant sources. The feasibility of this approach has been illustrated by numerical computations within Cartesian coordinates, using biophysically derived excitation equations for mammalian atrial and ventricular tissue, Biktashev and Holden [8], [9].

[★] To appear in *Chaos Solitons and Fractals*

¹ Author to whom correspondence should be addressed

The heart has a complicated, anisotropic and moving geometry [17], and as a step to modelling the endocardial surface of the atrium as a spherical surface we examine induced resonant drift of rigidly rotating spiral waves in circular and annular domains. A circular domain also provides a natural model for experiments on chemical excitable media in a thin film in a Petri dish *e.g.*, see Grill *et al* [16], Müller *et al* [20], and Gómez-Gesteira *et al* [15].

2 Model formulation

2.1 Mathematical model

We use the FitzHugh-Nagumo excitable media model in the form, Winfree [25],

$$\frac{\partial u}{\partial t} = D \nabla^2 u + \frac{f(u, v)}{\epsilon} + F(t), \quad \frac{\partial v}{\partial t} = \epsilon g(u, v), \quad (1)$$

where D is a diffusion coefficient, ∇^2 is the Laplacian, $F(t)$ is an external forcing, and the non-linear terms are

$$f(u, v) = u - \frac{u^3}{3} - v, \quad g(u, v) = u + \beta - \gamma v. \quad (2)$$

In polar coordinates r and φ the Laplacian reads

$$\nabla^2 = \frac{1}{r} \frac{\partial}{\partial r} \left(r \frac{\partial}{\partial r} \right) + \frac{1}{r^2} \frac{\partial^2}{\partial \varphi^2}. \quad (3)$$

The first equation in (1) describes the fast process of formation and propagation of the wave front; the second equation describes the local recovery of the properties of the medium. In the context of biological excitable tissues the variables u and v are commonly interpreted as the membrane potential of the cell, and the slow repolarizing currents through the membrane; the $F(t)$ can be interpreted as, for instance, an external electric current.

2.2 Boundary conditions

For a disk with radius R the nonflux boundary condition is posed

$$\left. \frac{\partial u}{\partial r} \right|_{(R, \varphi)} = 0, \quad 0 \leq \varphi \leq 2\pi. \quad (4)$$

In the case of an annulus, $r_h \leq r \leq R$, r_h is the hole radius, the nonflux boundary conditions are posed on both boundaries

$$\left. \frac{\partial u}{\partial r} \right|_{(r_h, \varphi)} = \left. \frac{\partial u}{\partial r} \right|_{(R, \varphi)} = 0, \quad 0 \leq \varphi \leq 2\pi. \quad (5)$$

2.3 Computational model

The system (1)-(5) was integrated, using a semi-implicit Euler method. A uniform rectangular grid with radial and angular steps $(\Delta r, \Delta \varphi)$ in a rectangle $\bar{G} = \{r_h \leq r \leq R, 0 \leq \varphi \leq 2\pi, r_h \geq 0\}$ was used. The derivatives with respect to r and φ were approximated by central differences, except for the radial derivative $\partial u / \partial r$ at the boundaries, where the one-sided second order differences were used

$$\left. \frac{\partial u}{\partial r} \right|_{(R, \varphi)} \approx \frac{1}{2\Delta r} (3u(R, \varphi) - 4u(R - \Delta r, \varphi) + u(R - 2\Delta r, \varphi)), \quad (6)$$

$$\left. \frac{\partial u}{\partial r} \right|_{(r_h, \varphi)} \approx \frac{1}{2\Delta r} (-3u(r_h, \varphi) + 4u(r_h + \Delta r, \varphi) - u(r_h + 2\Delta r, \varphi)). \quad (7)$$

To provide convergence at small r , the simplest implicit finite difference approximation of the angular part of the Laplacian was used. Both the radial part of the Laplacian and the non-linear terms were integrated explicitly. To resolve the resultant linear system a cyclic elimination method was implemented [24]. The Laplacian at $r=0$ was computed by formula (8) resulting from the mean value theorem for a disk [11], [22], [23],

$$\nabla^2 u(0) = \lim_{r \rightarrow 0} \frac{4}{r^2} \left(\frac{1}{2\pi} \int_0^{2\pi} u(r, \varphi) d\varphi - u(0) \right) \quad (8)$$

More precisely, the non-local boundary condition at $r = 0$ has been set

$$\nabla^2 u^{t+\Delta t}(r, \varphi)|_{r=0} = \frac{4}{\Delta r^2} \left(\frac{1}{M} \left(\sum_{j=1}^M u_{1j}^{t+\Delta t} \right) - u_0^{t+\Delta t} \right) \quad (9)$$

Here u_{1j}^t are the values of u at the circumference with radius Δr , M is the number of angular segments, and u_0^t is the value of u at $r = 0$.

2.4 Parameters

The model parameters $D = 1$, $\beta = 0.75$, $\gamma = 0.5$, and $\epsilon = 0.3$ were fixed to correspond to an excitable medium with a stable spatially uniform steady state that can support stable rigidly rotating spiral waves in the plane [25]. With the parameters chosen, the propagation velocity of a solitary plane wave is approximately 1.8 su/tu, where su = ‘space units’ and tu = ‘time units’. The wavelength of the spiral wave is 36.4 su, with the core radius of ~ 3.2 su, and its period is about 21.4 tu. Since we are interested in re-entrant cardiac arrhythmia the size of the circular domain, $R = 30$, has been chosen of the same order as the spiral wavelength. The hole radius was varied within $0 \leq r_h \leq 3.5$. In most of the computations the time step $\Delta t = 0.01$ and both space and angular steps $\Delta r = 0.2$, and $\Delta \varphi = 2\pi/600$ were fixed. To verify the robustness of the numerical results smaller time and space steps $\Delta t = 0.005$ and $\Delta r = 0.12$ were sometimes used.

2.5 Tip position, phase, and instantaneous frequency of wavetip rotation

The wave tip was found as the intersection of two isolines $u = v = 0$, by linear interpolation between their crossings of the mesh ribs. The phase Φ of the spiral wave was computed as $\Phi = \arctan\left(\frac{\partial v}{\partial y} / \frac{\partial v}{\partial x}\right)$ at the wavetip, according to the definition given in Biktashev *et al* [10]. This was obtained *via* the derivatives $\partial v / \partial r$ and $\partial v / \partial \varphi$ computed by central differences at the corners of the mesh cell containing the tip and then bilinearly interpolated to the tip point. The instantaneous frequency of wavetip rotation at time t was accepted as the value of $\omega = 2\pi/T$ with the least $T > 0$ satisfying the condition $\Phi(t) = \Phi(t + T) \pm 2\pi$.

2.6 External time forcing

The function $F(t)$, $0 \leq F(t) \leq A$, was a series of rectangular pulses of a fixed duration $\Delta t_{ef} = 0.1$ tu with amplitude A , $0 \leq A \leq 10$, varying in different numerical experiments. The time moments t_k , $k = 0, 1, \dots$, at which the perturbation of amplitude A and duration Δt_{ef} was applied were determined by one of the following procedures:

- (i) $t_k = kT_c + \tau$, where T_c was the constant period of $F(t) \equiv F(t + T_c)$ and τ was a time delay;
- (ii) $t_k = t_{\omega,k} + \tau$, where $t_{\omega,k}$ was the k -th moment in time t when the condition $\Phi(0) \equiv \Phi(t_{\omega,k}) \pmod{2\pi}$ had been fulfilled, $\Phi(0)$ was the phase at $t = 0$;
- (iii) $t_k = t_{re,k} + \tau$; here $t_{re,k}$ was the k -th moment in t when the excitation wavefront, the isoline $u = 0$, reached a control point interpreted as a recording electrode.

2.7 Initiation of spiral wave

To initiate a spiral wave rotating near the centre of a circular medium, as seen in Figure 1(a), an annulus with a small hole was used. Two thin adjacent radial slices of a width about 6° were set, one corresponding to an excitation state with $u = 2.0$ and $v = -0.65$; the other corresponding to a recovering state with $u = -2.0$ and $v = 0.67$; and the remainder of the annulus was set to the quiescent state, $u = -1.125$ and $v = -0.65$. These initial conditions gave rise to a rigidly rotating wave attached to the hole, with the direction of rotation determined by the order of the two slices. Setting the hole radius to $r_h = 0$ resulted in a spiral wave rigidly rotating around a point close to the centre of the medium. To obtain a spiral wave with the wave tip close to the boundary, as shown in Figure 1(b), external time forcing with a frequency equal to the instantaneous rotation frequency of the wave was used, see (ii) in Sect.2.6. The technique allowed us to place the core anywhere in the medium by choosing different a number of stimuli, delay τ and forcing amplitude A . An alternative way of spiral wave initiation can be found in, *e.g.* Zykov and Müller [26]. In all the numerical experiments described below spiral waves were rotating in the counter-clockwise direction.

2.8 Grid anisotropy

The grid spacing and time step were chosen to reliably create spiral waves with appropriately smooth profiles and propagation speeds. A criterion of numerical accuracy was that small changes in the grid or time step should not give rise to large differences in the solution. With numerical parameters chosen as in Sect.2.4 neither reducing the steps Δr or $\Delta \varphi$ by 20% nor reducing the time step by 50% changed the wave period by more than 2%. Nevertheless, even in the absence of any forcing, a radial drift of spiral waves away from the centre was observed. The radial drift velocity $v_a \sim 2.4 \cdot 10^{-3}$ su/tu was less than 0.2% of the plane wave velocity. Numerical experiments evidenced that the mentioned radial drift velocity decreased as the Δr became smaller,

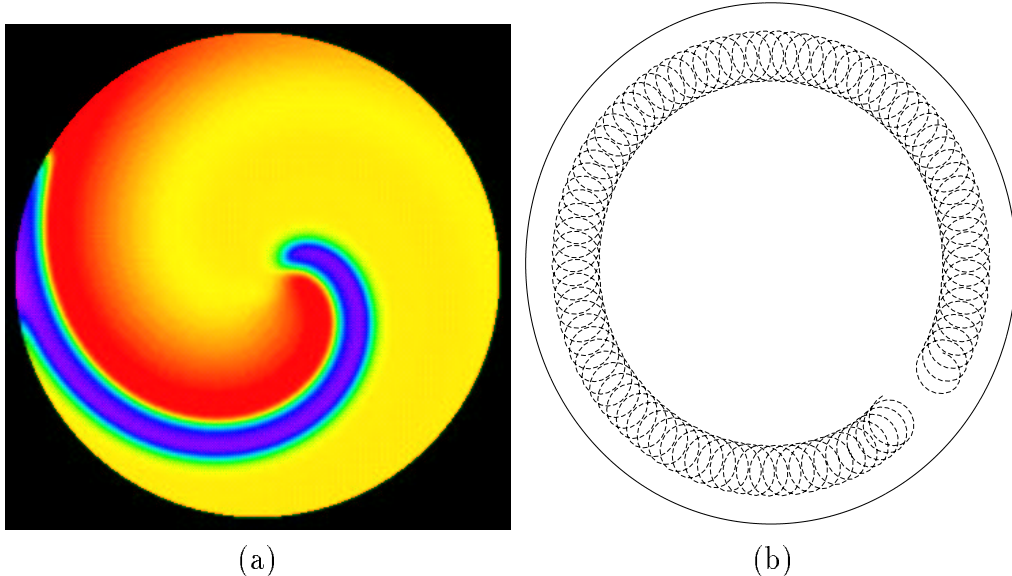


Fig. 1. (a) Colour visualization of the excitatory process u in a rigidly counter-clockwise rotating spiral wave with the core of radius ~ 3.2 space units in a circular domain of radius $R = 30$ space units. (b) Biperiodic motion, produced by boundary interactions. Shown is the tip trajectory of a counter-clockwise rotating spiral wave which drifts along the boundary in the clockwise direction.

$v_a \sim 4.8 \cdot 10^{-3}$ su/tu for $\Delta r = 0.4$; $v_a \sim 2.4 \cdot 10^{-3}$ su/tu for $\Delta r = 0.3$; $v_a \sim 1.2 \cdot 10^{-3}$ su/tu for $\Delta r = 0.2$; and $v_a \sim 3.5 \cdot 10^{-4}$ su/tu for $\Delta r = 0.1$. In these test computations the time step $\Delta r = 0.001$ was used to satisfy the stability criterion for the case of the smallest $\Delta r = 0.1$. The very slow radial drift should probably be attributed to the grid anisotropy produced by the summation of local errors of approximation in integrating the discrete analog of equations (1)-(5) in polar coordinates. In numerical experiments described below, this numerical artefact was always much smaller than the resonant drift.

3 Results

3.1 Constant frequency resonant drift

It has been long known that spatially uniform, periodic time forcing leads to the motion of a rigidly rotating spiral wave. If the frequency of forcing is close to the rotation frequency of the spiral wave, a circular, large radius “Larmor”-type drift results (motion equations of the rotation center are similar to those of a charged particle in a magnetic field); if the frequency is equal to the rotation frequency a linear, directed resonant drift in a direction determined by the phase of the forcing results, Agladze *et al.* [1]; Davydov *et al.* [13]; Biktashev and Holden [7]; Mantel and Barkley [18]. Figure 2 illustrates the

boundary interactions of a resonantly drifting spiral. The closer the resonantly drifting spiral wave approaches the boundary the faster the core rotates (see 2(b) and (d)), hence the greater the changes in the phase at which the constant frequency forcing is applied, and the greater the changes in the direction of the drift. Fig. 2a shows that the tip positions at which the forcing is applied move along a hypocycloid near the boundary. In Fig. 2(a) the rotation of the core and the boundary induced drift are opposite to each other while in (c) these coincide. Figures 2(e) and (f) illustrate the effects of internal boundaries, or holes in the medium. In (e) the resonantly drifting spiral is repelled by the hole of a similar size to the core of the wave, and in 2(f) is captured by the smaller hole.

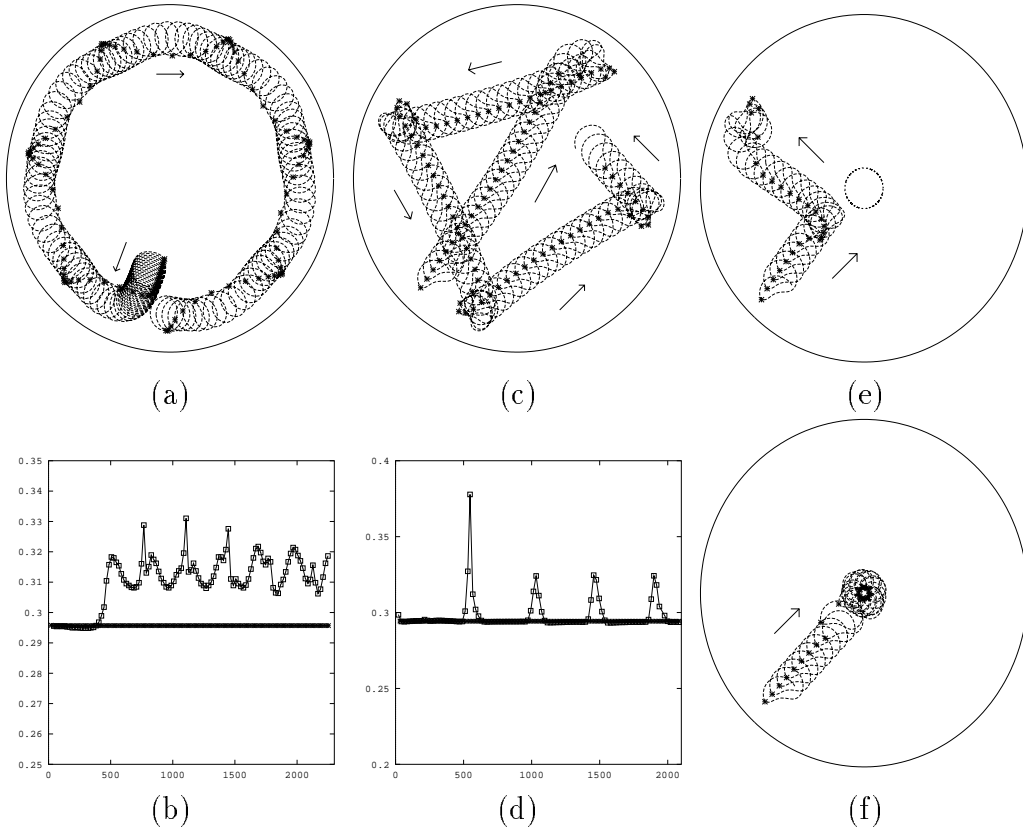


Fig. 2. Tip trajectory of a spiral wave with drift induced by spatially uniform periodic stimulation at a constant frequency. In (a), (c), (e), and (f) the * marks the position of the wavetip at the time when the perturbation is applied. (a) and (b) Stimulation with amplitude $A = 0.6$. (c)-(f) $A = 2.5$. (b) and (d) Dependencies of the instantaneous frequency of the spiral's wavetip rotation on time. "Squares" indicate the values of the instantaneous frequency of the spiral, and the * indicate the stimulation frequency; (b) corresponds to (a); (d) corresponds to (c). (e) Repulsion of the drifting spiral wave by an obstacle in the medium, a hole with radius $r_h = 3.5$. (f) Capture of the resonantly drifting spiral wave by a small hole of radius $r_h = 1$.

3.2 *Feedback resonant drift monitored by wavetip orientation*

An ideal way to avoid the resonant repulsion from the boundaries is to monitor the instantaneous frequencies of the rotation of the wave tip, as described in Sect.2.6, and thereby to apply the resonant forcing at exactly the same phase of resonantly drifting spiral each rotation [7]. Figure 3 illustrates the spiral wave response to a spatially uniform perturbation applied at the same phases of the rotating wave. In 3(a) the amplitude of the perturbation is insufficient to overcome the non-resonant interaction with the boundary, and the counter-clockwise rotating spiral drifts clockwise around the boundary, slowing down and finally freezing in position with its tip's trajectory approaching a cycle that does not move, where the effects of resonant forcing and the interaction with the boundary cancel each other. In 3(b) the amplitude of the perturbation is larger, the linear drift velocity is larger, and the spiral collides and is extinguished at the boundary. In 3(c) and (d) interactions with an interior obstacle, an inexcitable hole, are illustrated; in (c) the spiral is trapped around a small hole (whose diameter is less than the core diameter) and finally breaks free, and is extinguished at the boundary, while in 3(d) the spiral is trapped and bound by a hole that has a diameter larger than the spiral core diameter.

3.3 *Feedback resonant drift monitored by a recording electrode*

Another method, that is more appropriate for applications, is to monitor activity at a point in the medium, as if by a recording electrode. In this case both the position of the recording electrode and the time delay τ between recording wave arrival and stimulation are all arbitrary, but in fact turn out to be of great importance. Figure 4 illustrates the synchronization of the rotations of the core of the spiral by the resonant forcing, when the wavetip drifts around a stable limit cycle, a circle with a centre that coincides with the location of the recording electrode point; in (a) the symmetry center is the centre of the medium, in (b) the symmetry centre is shifted at the point with the radius $r_{re} = 10$. An increase of amplitude A results in an increase of the angular velocity of the drift along these circles, but does not influence their radii. Changing the time delay, one can change the radius and/or reverse the direction of the drift along the circle, in (a) the drift occurs in the counter-clockwise direction while in (b) in the opposite direction. All this is consistent with the phenomenological theory of the resonant drift described in [7]. Indeed, the equations (63) therein, that describe the feedback-driven resonance drift in the absence of interactions with the boundary, can be rewritten in the form

$$\dot{\rho} = c \cos(\Psi(\rho)), \quad \dot{\varphi} = \frac{c}{\rho} \sin(\Psi(\rho)), \quad (10)$$

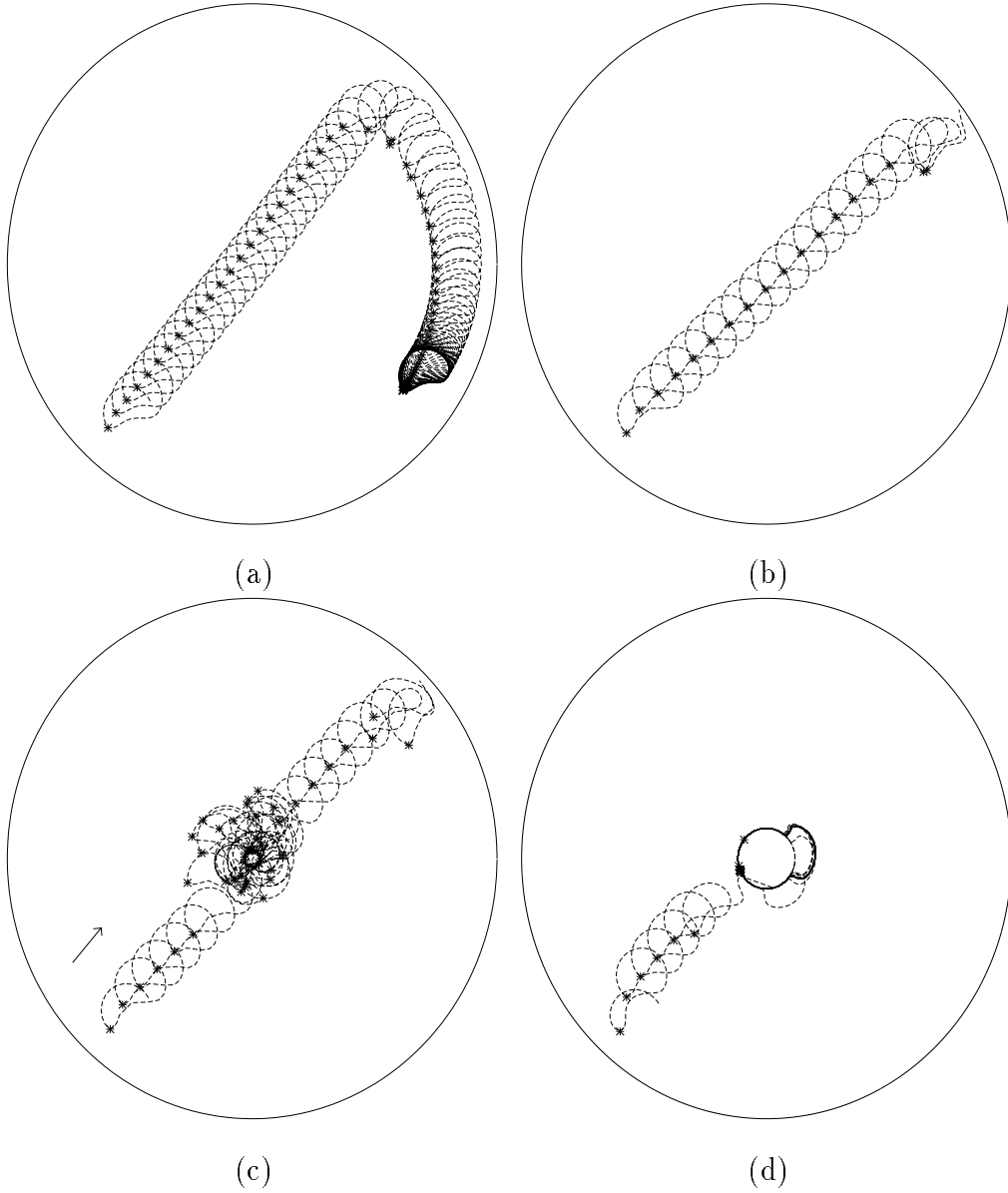


Fig. 3. Feedback resonant drift produced by spatially uniform, repetitive stimulation controlled by monitoring the wavetip orientation. Amplitude of perturbation $A = 2.5$ in (a), and $A = 3$ in (b)-(d). The * marks the position of the wave's tip at which the perturbation is applied. (a) Stimulation amplitude is not large enough to extinguish the resonantly drifting spiral wave, and the core moves around the boundary, and is finally frozen at the boundary. (b) Resonantly drifting spiral wave is extinguished at the boundary by the higher amplitude stimulation. (c) Resonantly drifting spiral wave attaches to, and is detached from, a small hole with radius $r_h = 1$, and finally collides with, and is extinguished at, the boundary. (d) Resonantly drifting spiral wave becomes attached and bound to a hole with radius $r_h = 3.5$.

where (ρ, φ) are polar coordinates of the spiral wave core, $\rho = 0$ corresponds to the recording electrode; $\Psi(\rho) = 2\pi(\rho/\Lambda + \tau/T)$, Λ and T are the asymptotic wavelength and the period of the wave respectively, and τ is the stimulation delay; c is a constant determined by the forcing amplitude A . Equations (10) admit a discrete family of limit cycles

$$\rho(t) = \Lambda((2m + 1)/4 + \tau/T), \quad \varphi(t) = (-1)^m ct/\rho, \quad m = 0, 1, 2, \dots (11)$$

Thus the feedback results in a synchronization of the tip motion by the external stimuli so that, after some transient process, the wavetip approaches a closed circular trajectory centered at the measuring point. This leads to an idea of extinguishing the resonantly drifting spiral wave near the boundary by resonant drift along a circular arc which would intersect the boundary. To do this one could set the recording electrode at the boundary as proposed in [7].

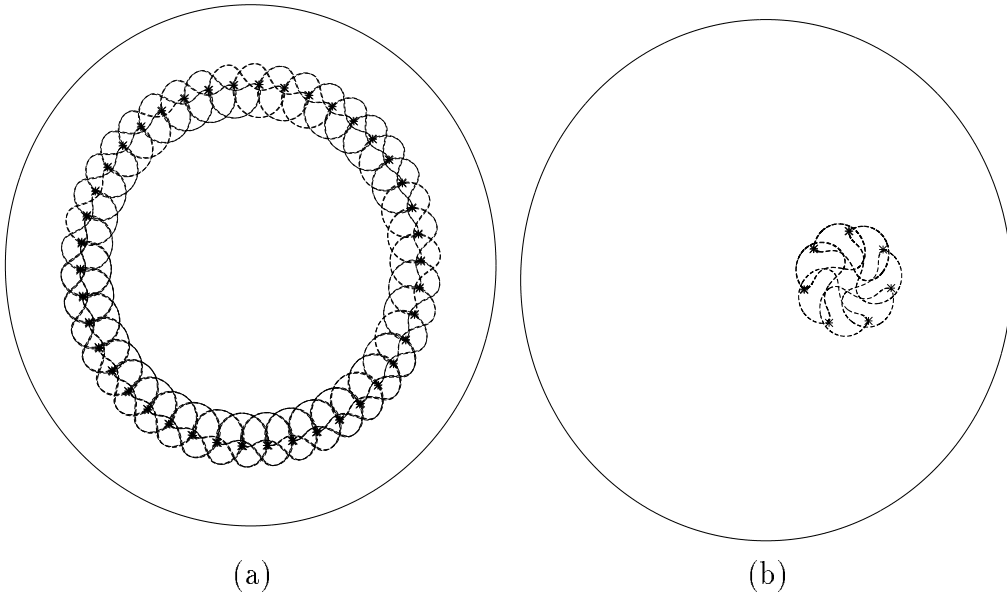


Fig. 4. Tip trajectories computed under feedback control by a recording electrode sited at the centre, $r_{re} = 0$, of the medium in (a) and at $r_{re} = 10$ in (b). Amplitude of stimulation $A = 3$. In both (a) and (b) the spiral waves are rotating counter-clockwise.

Figure 5 illustrates the process of extinguishing the spiral waves in the case when the recording electrode is set at the boundary. Most of the core trajectories do not resemble circular arcs because the core reaches the boundary during the transient processes. Notice that the shape of these trajectories before touching the boundary is similar to those obtained in square media, see Figure 14 in [7].

We have seen that drift along a circular trajectory can occur in the absence of interaction with boundaries due to the symmetry of drift motion equations. However, similar drift can occur even in case of strong interaction with

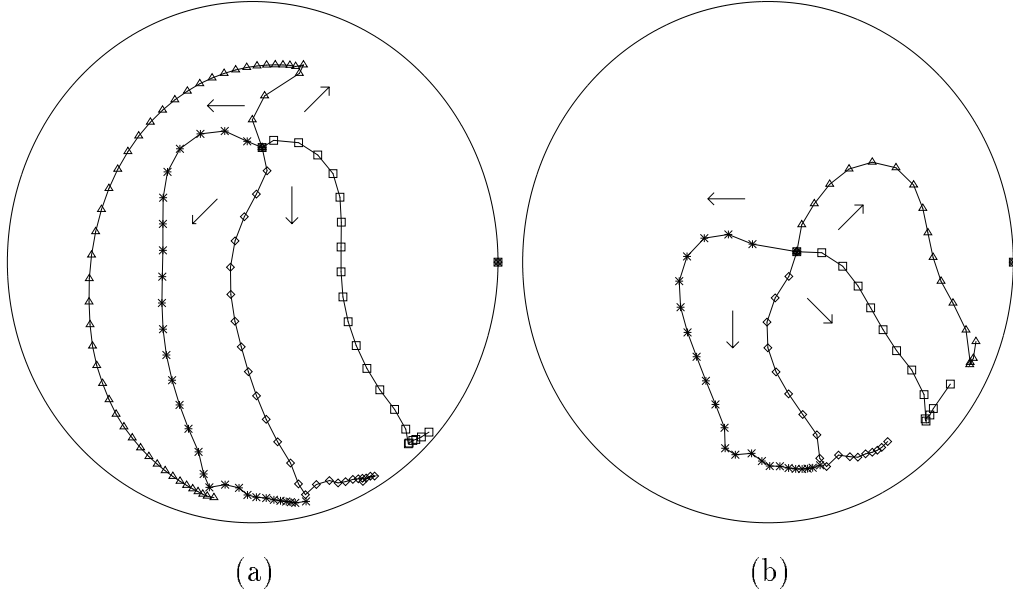


Fig. 5. Resonant drift under feedback control by a recording electrode, the perturbation of amplitude $A = 3$ is applied at fixed time after the wavefront reaches the recording site. The four wave's core trajectories correspond to different initial wave's phases, 0 , $\frac{\pi}{2}$, π , and $\frac{3\pi}{2}$, at which the first perturbation pulse was applied. Shown are positions of the tip at the times the perturbations were applied. The solid circle marks the recording site.

boundary. In Fig. 6(a), the resonantly drifting spiral wave is first pushed to and then moves along a circular trajectory clockwise around the boundary, increasing in drift velocity as it approaches the recording site. When the spiral tip comes close to the recording site, the tip is detached from the boundary and moves along a smaller circular trajectory inside the medium, this time counter-clockwise, then attaches to the boundary and follows the boundary in a circular clockwise motion and finally freezes. These nearly circular motions along the boundary result from the small difference between the perturbation frequency and the spiral wavetip frequency seen in Figures 6(b), which in turn is related to the fact that in the absence of forcing, the drift due to interaction with boundary is also circular, as shown in Fig. 1(b). This interpretation is confirmed by the next numerical experiment shown in Fig. 6(c),(d), which stimulated a similarly complicated shape of trajectory by varying the stimulation protocol. First, the spiral wave was set to drift clockwise along the boundary without external forcing (left half of medium in Fig. 6(c)). Then a feedback-driven forcing was started (shown by asterisks), which led to detaching the spiral wave from the boundary and to its drift counterclockwise through the interior of the medium, until reaching the boundary again, which ended this time up with extinguishing the spiral wave.

Figure 7 illustrates interactions between resonant drift under feedback control and an inexcitable hole; in (a) the tip trajectory is trapped by the small hole, and breaks free, to be extinguished at the boundary; in (b) the spiral

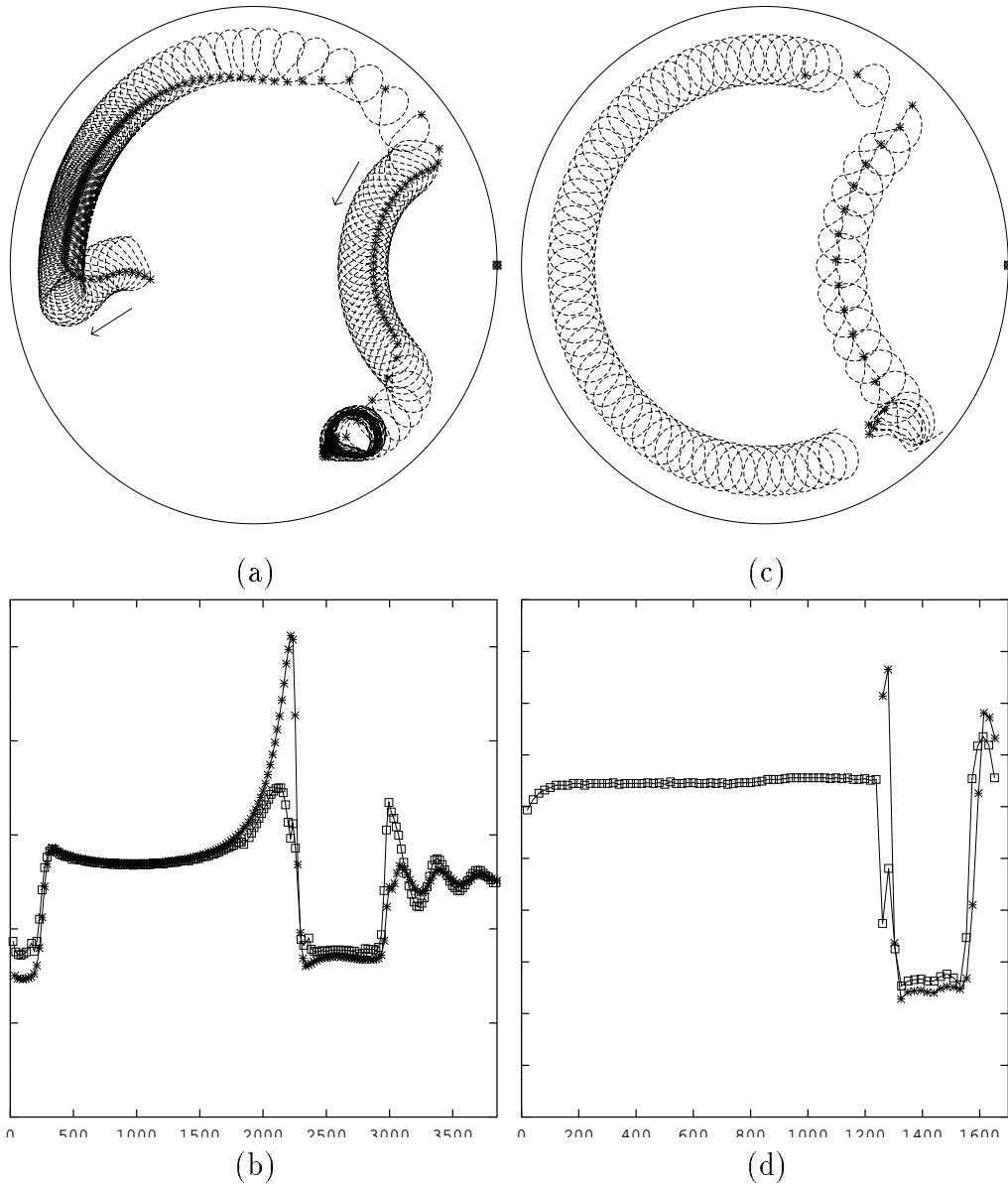


Fig. 6. A complicated sequence of spiral wave boundary interactions, with resonant drift under feedback control by a recording electrode, repetitive stimulation with uniform amplitude $A = 2.5$ in (a),(b) and $A = 3$ in (c),(d). The * marks the positions of the spiral's wavetip at the time moments when the perturbation is applied; the solid circle marks the recording site. (a) Tip trajectory of the resonantly drifting wave, which is first driven towards the boundary, moves circumferentially around the boundary, gradually speeding up, until it is repelled from the boundary and undergoes a Larmor-type drift before returning to the boundary and finally being frozen at the boundary. (b) Dependence of the instantaneous frequency of the spiral's wavetip (marked by the squares) and the frequency of stimulation (marked by the *) on time. (c) Shown is the tip trajectory of a spiral wave drifting clockwise along the boundary in the absence of any external forcing, the left part of the figure; when external forcing is turned on, the trajectory executes a nearly circular motion around the recording electrode site, the right part of the figure. (d) Dependence of the instantaneous frequency of the rotation of the spiral's wavetip motion of 6(c) (marked by the squares) and the frequency of stimulation (marked by the *) on time.

wave is trapped and is bound to the larger hole, while in (c) and (d) the tip trajectory bypasses the hole and the spiral wave is extinguished. This confirms the importance of the time delay parameter in the feedback controlled resonant drift. An appropriately chosen time delay parameter allows the resonantly drifting spiral waves to bypass the obstacle and reach the boundary where it is finally extinguished.

4 Conclusion and discussion

We have presented numerical results on the resonant drift of rigidly rotating spiral waves within a circular domain, and interaction of resonantly drifting spiral waves with medium obstacles and boundaries. We have considered media with a radius the same order of magnitude as the spiral wavelength, and the simplest possible spiral wave motions, a periodic rigidly rotating wave and a bi-periodic one, drifting along the boundary. In the context of applications to cardiac arrhythmia, the rigidly rotating wave corresponds to a re-entrant propagation of the leading circle type, around a functional block (the core, in spiral wave terminology), while the bi-periodic motion corresponds to re-entrant wave around an anatomical obstacle, such as the inferior vena cava in a right atrial flutter. Both types of re-entry were subjected to both a constant periodic and feedback controlled resonant external time forcing.

Although a circular domain provides a more natural model for cardiac tissue than a rectangular domain, special care should be taken in carrying out numerical experiments in polar coordinates to study the drift phenomenon. As mentioned in Sect.2.8, integration in polar coordinates shows a very slow radial drift of spiral waves even in the absence of external forcing. Such a slow drift has been described in experiments with the Belousov-Zhabotinsky reaction, Gómez-Gesteira *et al* [15], however, in the numerical experiments it is a numerical artefact, as its velocity varies with the step size, and is due to grid anisotropy caused by nonuniform errors of the finite difference approximation of the original equations.

Earlier work on the effects of periodic forcing on spiral waves has been by a kinematic approach Davydov *et al* [13] and Mikhailov *et al* [19], by numerical, phenomenological and asymptotical studies by Biktashev and Holden [4]-[9], and by the forcing of a model ODE system by Mantel and Barkley [18]. These studies provide insight into the directed motion or resonant drift of spiral waves, and in the context of cardiac defibrillation deal with moving the re-entrant wave towards a boundary. Interactions with a boundary have not been so intensively studied - however see Biktashev [3], Ermakova *et al* [14], Aranson *et al* [2] and Biktashev and Holden [7], and the implicit assumption is that the spiral will either be reflected or extinguished at the boundary. For

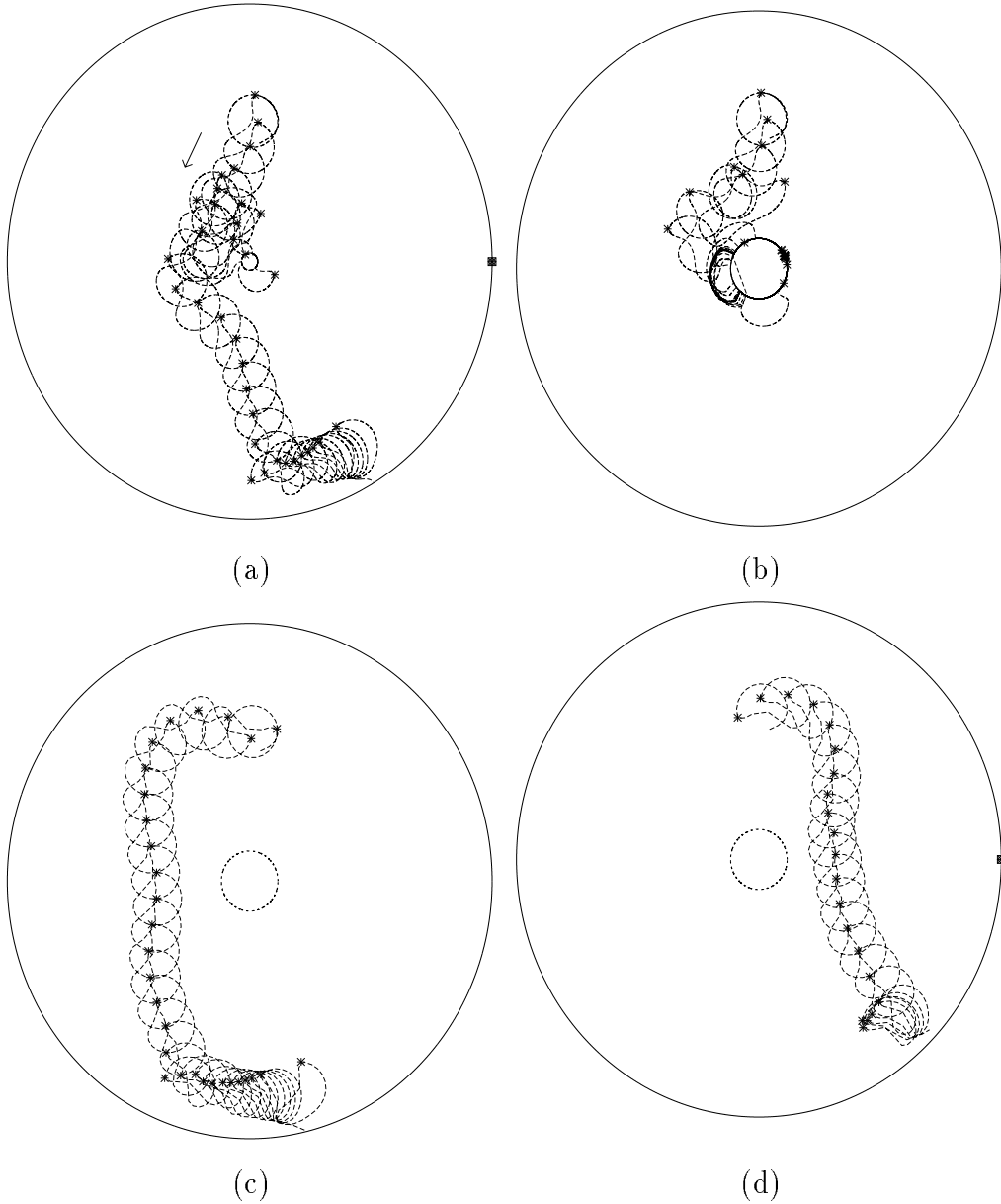


Fig. 7. Resonant drift under feedback control by a recording electrode in circular media with circular obstacles and perturbations of amplitude $A = 3$. The * marks the position of the spiral's wavelip at the time when the perturbation is applied; the solid circle marks the recording site. (a) Hole with radius $r_h = 1$ being less then the wave's core size. (b)-(d) Hole with radius $r_h = 3.5$ of the same order as the core of the unperturbed spiral. Initial wave's phases at which the first stimulation was applied are 0 in (c), $\frac{\pi}{2}$ in (b), and π in (d).

the purposes of efficient extinction of spiral wave at the medium boundary it is of great importance to understand possible types of spiral wave behavior near the boundary.

Biktashev and Holden [4]-[9] used resonant drift under feedback control to

overcome boundary interactions, with the feedback triggered by a recording electrode located in a corner of the medium. If the recording electrode is located within the interior of the circular domain then, independently of however far from the wavetip of a rigidly rotating wave it is located, synchronization of the tip motion occurs and after a transient the wavetip approaches a closed circular trajectory centered at the recording electrode point, Figure 4. An analogous synchronization phenomenon has been observed earlier in the case of meandering spiral waves in Grill *et al.* [16]. Thus the recording electrode feedback stimulation produces a synchronized dynamical behavior for the cases of rigidly rotating or meandering spiral waves, and the case of biperiodic motion near the boundary within a circular medium. The recording electrode imposes a centre of symmetry for the system. Motion is a circle around the recording electrode. Since simple re-entry in the wall of a heart chamber occurs in an anatomically defined, complicated three-dimensional structure some locations for a recording electrode used to control re-entrant activity by resonant drift will be more effective than others in driving re-entrant activity to a boundary with inexcitable tissue.

When interaction between the drifting spiral wave and inexcitable obstacles in the medium traps the spiral wave, as in the pinning described by Davidenko *et al* [12], recording electrode feedback-controlled forcing can, in some (see Fig. 7(a)), but not all cases (see Fig. 7(b)) , detach the spiral from the obstacle. Even in the cases when the wavetip could not be detached from the obstacle by recording electrode feedback-controlled forcing a properly chosen delay allowed one to manage the drift in such a way to avoid the obstacle and finally successfully extinguish the wave at the boundary, Fig. 7c,d. If the obstacle is an anatomical obstacle in the heart, then choice of recording site and time delay could, in principle, produce resonantly drifting trajectories that avoid the obstacle.

Acknowledgement

This work was supported in part by The Wellcome Trust (045192) and EPSRC-ANM (GR/K49775) grants.

References

- [1] K.I. Agladze, V.A. Davydov and A.S. Mikhailov, An observation of resonance of spiral waves in distributed excitable medium. *ZETP Lett* **45**, 767-770 (1987).
- [2] I. Aranson, D. Kessler and I. Mitkov, Drift of spiral waves in excitable media. *Physica-D* **85**, 142-155 (1995).

- [3] V.N. Biktashev, Drift of a reverberator in an active medium due to interaction with boundaries, in *Nonlinear Waves II Dynamics and Evolution*, Edited by A.V. Gaponov-Grekhov, M.I. Rabinovich and J. Engelbrecht, pp.87-96. Springer, Berlin (1989).
- [4] V.N. Biktashev, Control of re-entrant vortices by electrical stimulation, in *The Computational Biology of the Heart*, Edited by A.V. Panfilov and A.V. Holden. John Wiley, Chichester (1997).
- [5] V.N. Biktashev and A.V. Holden, Resonant drift of an autowave vortex in a bounded medium. *Phys Lett A* **181**, 216-224 (1993).
- [6] V.N. Biktashev and A.V. Holden, Design principles of a low voltage cardiac defibrillator based on the effect of feedback resonant drift. *J. Theor. Biol* **169**, 101-112 (1994).
- [7] V.N. Biktashev and A.V. Holden, Resonant drift of autowave vortices in two dimensions and the effects of boundaries and inhomogeneities. *Chaos, Solitons and Fractals* **5**, 575-622 (1995).
- [8] V.N. Biktashev and A.V. Holden, Control of re-entrant activity in a model of mammalian atrial tissue. *Proc. Roy. Soc. Lond.* **B260**, 211-217 (1995).
- [9] V.N. Biktashev and A.V. Holden, Re-entrant activity and its control in a model of mammalian ventricular tissue. *Proc. Roy. Soc. Lond.* **B 263**, 1378-1382 (1996).
- [10] V.N. Biktashev, A.V. Holden and E.V. Nikolaev, Spiral wave meander and symmetry of the plane. *Int.J.Bif.and Chaos* **6(12)**, (1996).
- [11] R. Courant and D. Hilbert, *Methods of Mathematical Physics*. J.Wiley & Sons, New York (1962).
- [12] J.N. Davidenko, A.M. Pertsov, R. Salomonsz, W. Baxter and J. Jalife, Stationary and drifting spiral waves of excitation in isolated cardiac muscle. *Nature* **335**, 349-351 (1992).
- [13] V.A. Davydov, V.S. Zykov, A.S. Mikhailov and P.K. Brazhnik, Drift and resonance of spiral waves in distributed media. *Izv. Vuzov-Radiofizika* **31**, 574-582 (1988).
- [14] E.A. Ermakova, A.M. Pertsov and E.E. Shnol, On the interaction of vortices in two-dimension media. *Physica D* **40**, 185-190 (1989)
- [15] M. Gómez-Gesteira, A.P. Muñuzuri, V. Pérez-Muñuzuri and V. Pérez-Villar, Boundary imposed spiral drift. *Physical Rev E* **53**, 5480-5483 (1996).
- [16] S. Grill, V.S. Zykov and S.C. Müller, Feedback-controlled dynamics of meandering spiral waves. *Phys Rev Lett* **75(18)**, 3368-3371 (1995).
- [17] A.V. Holden, M. Markus and H.G. Othmer (eds.), *Nonlinear Wave Processes in Excitable Media*. Plenum Press Inc., New York (1991).

- [18] R.M. Mantel and D. Barkley, Periodic forcing of spiral waves in excitable media. *Phys. Rev. E* **54**, 4791-4802 (1996).
- [19] A.S. Mikhailov, V.A. Davydov and V.S. Zykov, Complex dynamics of spiral waves and motions of curves. *Physica-D* **70**, 1-39 (1994).
- [20] S.C. Müller, A. Warda and V.S. Zykov, Spiral Waves in Bounded Excitable Media, in *Modelling the Dynamics of Biological Systems. Nonlinear Phenomena and Pattern Formation*, Edited by E. Mosekilde and O.G. Mouritsen, pp. 7-22. Springer, Berlin (1995).
- [21] A.V. Panfilov and A.V. Holden (eds.), *The Computational Biology of the Heart*. John Wiley, Chichester (1997).
- [22] A.M. Pertsov, E.A. Ermakova and A.V. Panfilov, Spiral waves rotating around a hole, and vortices in a FitzHugh-Nagumo model. Preprint, Institute of Chemical Physics, USSR Academy of Sciences, Chernogolovka, Moscow Region (1983) (*in Russian*).
- [23] A.M. Pertsov, E.A. Ermakova and A.V. Panfilov, Rotating spiral waves in a modified FitzHugh-Nagumo model. *Physica* **14D**, 117-124 (1984).
- [24] A.A. Samarskii and E.S. Nikolaev, *Numerical Methods for Grid Equations*, Vol.I. Birkhäuser Verlag, Basel-Boston-Berlin (1989).
- [25] A.T. Winfree, Varieties of spiral wave behavior: An experimentalist's approach to the theory of excitable media, *Chaos* **1**, 303-334 (1991).
- [26] V.S. Zykov and S.C. Müller, Spiral waves on circular and spherical domains of excitable medium, *Physica* **97D**, 322-332 (1996).